

Simulation-Based Engineering Lab
University of Wisconsin–Madison

Technical Report TR-2016-11

Chrono Support for ANCF Finite Elements:
Formulation and Validation Aspects

Antonio Recuero and Dan Negrut

November 4, 2016

Abstract

This technical report describes the fundamentals of the nonlinear finite element theory used to implement ANCF finite elements in **Chrono**. The finite elements addressed in this document are: the gradient-deficient (cable) ANCF beam element, the 3-node shear deformable beam element, and the bi-linear laminated shell element with orthotropic material properties. The 3-node shear deformable ANCF beam element can be used for any application in which shear deformation, torsion, and/or bending are of interest. The ANCF shell element is also gradient deficient, as it only has one single gradient vector, and implements finite element numerical techniques to avoid kinematic locking, namely the assumed natural strain (ANS) and the enhanced assumed strain (EAS).

Keywords: 3-node shear deformable ANCF element, ANCF cable element, Laminated ANCF shell element, validation of finite elements, **Chrono** , open-source code

Contents

1	Introduction	3
2	ANCF Cable Element	4
2.1	Elastic Forces	5
2.2	Inertia Forces	5
3	Shear Deformable ANCF Beam Element	6
3.1	Elastic Forces	6
3.1.1	Structural Mechanics	6
3.1.2	Continuum Mechanics	8
4	Bilinear ANCF Shell Element	8
4.1	Computation of Strains for Curved, Orthotropic Shells	10
4.2	ANCF Shell Element Implementation	11
4.2.1	Initial Steps	11
4.2.2	Locking Remedies - Enhanced Assumed Strain	11
4.2.3	Locking Remedies - Assumed Natural Strain	12
4.2.4	Equations of Motion	13
4.3	Computation of the Jacobian of the Elastic Forces	13
5	Validation of Cable Element	14
5.1	Model's Definition	14
5.2	Numerical Validation	14
6	Validation of Beam Element	16
7	Validation of the ANCF Shell Element	16
7.1	Validation of the Isotropic Implementation	16
7.1.1	Model's Definition	16
7.1.2	Numerical Validation	16
7.2	Validation of the Orthotropic Implementation	18
7.2.1	Model's Definition	18
7.2.2	Numerical Validation	18

1 Introduction

The absolute nodal coordinate formulation (ANCF) is a nonlinear finite element formulation originated in the field of flexible multibody dynamics to describe large deformation of moving bodies. This formulation was introduced by Shabana [7] and contrasted with the co-rotational or floating frame of reference formulations because no co-rotated frame was used to describe the kinematics of deformed finite elements. Arguably, the most distinguishing feature of ANCF is the use of position vector gradients to describe the rotation of the body as well as its strain state, thereby avoiding the need for interpolating non-vectorial rotation parameters [5]. Without intention of completeness, we present a summary of the method in this section.

ANCF uses nodal, global position and position vector gradient vectors to describe the dynamics of flexible bodies that can experience large (as opposed to small) deformation; some authors identify this deformation magnitude as “moderate”, leaving the term “large” for massive deformation, e.g. for Eulerian-like approaches where the material flows. In general, the position field of an ANCF element may be defined as

$$\underbrace{\mathbf{r}^i(\xi, \eta, \zeta, t)}_{\text{Position of an arbitrary point within the element}} = \underbrace{\mathbf{S}(\xi, \eta, \zeta)}_{\text{Space-dependent shape function}} \times \underbrace{\mathbf{q}^i(t)}_{\text{Vector of nodal degrees of freedom}} \quad (1)$$

where i is an arbitrary finite element, ξ, η, ζ are local element parameters, t is the time, \mathbf{S} a matrix of shape functions, and \mathbf{q}^j is a vector containing nodal coordinates.

One classification for ANCF elements may be based on the number of position vector gradients per node, as follows:

- **Fully parameterized.** These ANCF finite elements possess a full set of gradient vectors, that is, each node has one position vector \mathbf{r} , and three position vector gradients $\mathbf{r}_x, \mathbf{r}_y,$ and \mathbf{r}_z . Fully parameterized elements can straightforwardly implement continuum mechanics approaches, which usually rely on deformation gradient tensors, \mathbf{F} .
- **Gradient deficient.** Many ANCF finite elements do not have a full set of gradients for several reasons; e.g. one or two position vector gradients may suffice to define a volume and, therefore, to use a continuum mechanics approach. Further, the use of a class of gradient-deficient elements has been found to successfully eliminate diverse locking problems (poor description of elemental strain state).
- **Higher-order coordinates.** Finite element technology allows the use of higher-order derivatives of position vectors as nodal coordinates. This has found to be beneficial to employ description of strains based on continuum mechanics [8].

There is an extensive body of literature that deal with the development of ANCF finite elements, including beams, shells, plates, and solids. Here, we are only going to summarize the formulation of three ANCF finite elements implemented in Chrono.

2 ANCF Cable Element

The ANCF cable element implemented in *Chrono* is a gradient-deficient element that was introduced by Berzeri and Shabana [2]. This beam element, often called “cable” element, consists of two nodes which have a position vector and a position vector gradient along the beam center axis as coordinates (see Fig. 1). The coordinates of a node k may be expressed as $\mathbf{q}^k(t) = [\mathbf{r}^{kT} \quad \mathbf{r}_x^{kT}]^T$. The position field of the ANCF beam element is defined as

$$\mathbf{r}^i = [s_1 \mathbf{I} \quad s_2 \mathbf{I} \quad s_3 \mathbf{I} \quad s_4 \mathbf{I}] [\mathbf{q}^{1T} \quad \mathbf{q}^{2T}]^T = \mathbf{S}(\xi) \mathbf{q}^i, \quad (2)$$

where the vector \mathbf{q}^i has the coordinates of both nodes, and the shape functions are defined as

$$\begin{aligned} s_1 &= 1 - 2\xi^2 + 2\xi^3, \\ s_2 &= l(\xi - 2\xi^2 + \xi^3), \\ s_3 &= 3\xi^2 - 2\xi^3, \\ s_4 &= l(-\xi^2 + \xi^3), \end{aligned} \quad (3)$$

where ξ is a local, adimensional parameter of the element that locates a point along the cable centerline ($\xi = 0$ at the first node), and l is the finite element’s reference length.

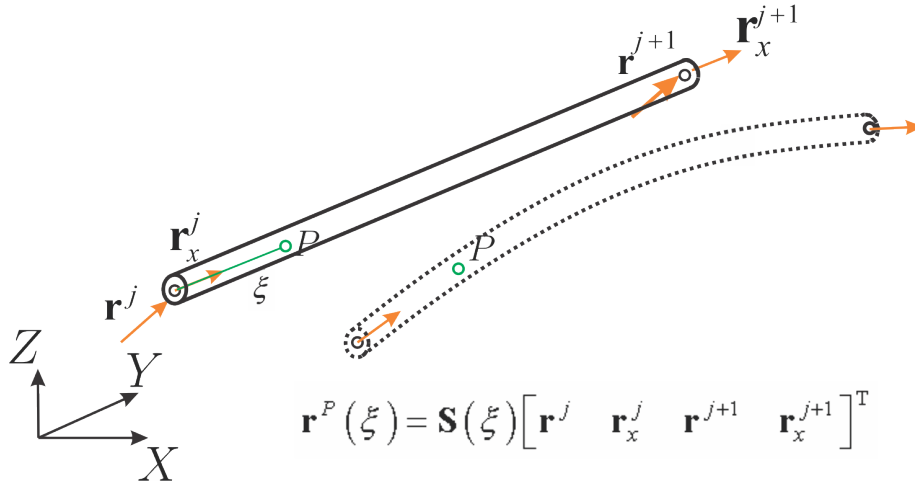


Figure 1: ANCF cable element’s kinematic description. ξ identifies a point P within the element.

2.1 Elastic Forces

Two strains fully define the internal forces of this element: the longitudinal stretch, ε_x , and the curvature, κ . The virtual work exerted by the internal forces may be written as follows

$$\delta W_e = \int_L [EA\varepsilon_x\delta\varepsilon_x + EI\kappa\delta\kappa]dx, \quad (4)$$

where E , A , and I are the modulus of elasticity, the cross section area, and the area moment of inertia, respectively; the longitudinal stretch and curvature are

$$\varepsilon_x = \frac{1}{2} (\mathbf{r}_x^T \mathbf{r}_x - 1) \quad \text{and} \quad \kappa = \frac{|\mathbf{r}_x \times \mathbf{r}_{xx}|}{|\mathbf{r}_x|^3},$$

respectively, where $\mathbf{r}_{xx} = \partial^2 \mathbf{r} / \partial x^2$. Note that the kinematics of this element cannot describe torsion or shear deformation. In addition, the cross section geometry is assumed axisymmetric.

2.2 Inertia Forces

The inertia forces take a simple form in ANCF; this is due to the description of bodies' kinematics directly in global coordinates. The velocity of any point within an element i may be written as

$$\underbrace{\dot{\mathbf{r}}^i(\xi, \eta, \zeta, t)}_{\text{Velocity of an arbitrary point within the element}} = \underbrace{\mathbf{S}(\xi, \eta, \zeta)}_{\text{Space-dependent shape function}} \times \underbrace{\dot{\mathbf{q}}^i(t)}_{\text{Vector of generalized velocities}}. \quad (5)$$

The kinetic energy of a finite element i may be obtained as

$$T = \frac{1}{2} \int_V \rho \dot{\mathbf{r}}^i{}^T \dot{\mathbf{r}}^i \, dV = \frac{1}{2} \dot{\mathbf{q}}^i{}^T \mathbf{M} \dot{\mathbf{q}}^i. \quad (6)$$

The mass matrix is defined as $\mathbf{M} = \int_A \rho A \mathbf{S}^T \mathbf{S} \, dx = \text{constant}$. By analyzing Eqs. (2.1) and (6), the reader may realize that the computation of inertia forces is much simpler than that of internal forces. This observation is valid not only for the beam element presented in this section, but for all ANCF finite elements: *Mass matrix is constant but the internal forces depend heavily nonlinearly on the coordinates*. It may also be noted that this particular ANCF beam element assumes that the section is axisymmetric, that is, the cross section properties are assumed to be same along any axis.

The Jacobian of the elastic forces is needed for the solution of index-3 DAEs in Chrono using implicit numerical integrators. Currently, this Jacobian is computed numerically via finite differences.

3 Shear Deformable ANCF Beam Element

The element described in this section and implemented in **Chrono** was proposed by Nachbagauer et al in [6]. It has three nodes and employs quadratic interpolation of three sets of variables: Position and two position vector gradients defining the cross section plane. This finite element has been demonstrated to yield accurate results for small and large deformation using two different internal force definition: Continuum-based and structural mechanics-based. The continuum-based flavor is implemented in **Chrono**.

The position of a material point P in this beam element is given by

$$\mathbf{r} = [s_1 \mathbf{I} \quad s_2 \mathbf{I} \quad \dots \quad s_9 \mathbf{I}] \begin{bmatrix} \mathbf{r}^1 \\ \mathbf{r}_y^1 \\ \dots \\ \mathbf{r}_z^3 \end{bmatrix}, \quad (7)$$

where \mathbf{r}^i , \mathbf{r}_y^i , and \mathbf{r}_z^i are the three sets of coordinate vectors of node i (see Fig. 2). The shape functions take the form of a quadratic polynomial along the length of the beam element and linear interpolation over the cross section, as follows:

$$\begin{aligned} s_1 &= -\frac{\xi}{2}(1 - \xi), \quad s_2 = \eta s_1, \quad s_3 = \zeta s_1 \text{ [First node]}, \\ s_4 &= \frac{\xi}{2}(1 + \xi), \quad s_5 = \eta s_4, \quad s_6 = \zeta s_4 \text{ [Second node]}, \\ s_7 &= -(\xi - 1)(\xi + 1), \quad s_8 = \eta s_7, \quad s_9 = \zeta s_7 \text{ [Third node]}. \end{aligned}$$

3.1 Elastic Forces

3.1.1 Structural Mechanics

In the structural mechanics flavor, at each beam cross section, a local material frame is created:

$$\mathbf{e}_1 = \frac{\mathbf{e}_1}{|\mathbf{e}_1|}, \quad \mathbf{e}_1 = \mathbf{r}_y \times \mathbf{r}_z; \quad \mathbf{e}_3 = \frac{\mathbf{e}_3}{|\mathbf{e}_3|}, \quad \mathbf{e}_3 = \mathbf{r}_z; \quad \mathbf{e}_2 = \frac{\mathbf{e}_2}{|\mathbf{e}_2|}, \quad \mathbf{e}_2 = \mathbf{r}_z \times (\mathbf{r}_y \times \mathbf{r}_z); \quad (8)$$

the local cross section frame used to define strains is then simply given by

$$\mathbf{A}_{cs} = [\mathbf{e}_1 \quad \mathbf{e}_2 \quad \mathbf{e}_3]. \quad (9)$$

Results from Eq. (8) are used to obtain axial and shear strains, as follows:

$$\Gamma_1 = \mathbf{e}_1^T \mathbf{r}_x - 1, \quad \Gamma_2 = \mathbf{e}_2^T \mathbf{r}_x - 1, \quad \Gamma_3 = \mathbf{e}_3^T \mathbf{r}_x - 1, \quad \mathbf{r}_x = \partial \mathbf{r} / \partial x, \quad (10)$$

3.1.2 Continuum Mechanics

The elastic energy, to be used to obtain generalized internal forces, may then be written as:

$$U^{CB} = \frac{1}{2} \int_{-W/2}^{W/2} \int_{-H/2}^{H/2} \int_{-L/2}^{L/2} \boldsymbol{\varepsilon}^T \boldsymbol{\sigma} \det(\mathbf{J}) \, dx dy dz \quad (13)$$

where $\boldsymbol{\varepsilon}$ is the vector of six strains (three axial, three shear) and $\boldsymbol{\sigma}$ is the stress tensor. This stress tensor is, in this formulation, the second Piola-Kirchhoff, which is conjugate to the Green-Lagrange strain tensor. The Poisson ratio ν couples ε_{xx} with ε_{yy} and ε_{zz} . This coupling, if integrated over the volume of this element, causes unwanted stiffness of the bending mode -that is, locking. To avoid this, one type of selective integration is used:

$$U_{SI}^{CB} = \frac{1}{2} \int_{-W/2}^{W/2} \int_{-H/2}^{H/2} \int_{-L/2}^{L/2} \boldsymbol{\varepsilon}^T \mathbf{D}^0 \boldsymbol{\varepsilon} \det(\mathbf{J}) \, d\xi d\eta d\zeta + \frac{1}{2} HW \int_{-L/2}^{L/2} \boldsymbol{\varepsilon}^T \mathbf{D}^\nu \boldsymbol{\varepsilon} \det(\mathbf{J}) \, d\xi \quad (14)$$

In which

$$\mathbf{D} = \underbrace{\mathbf{D}^0}_{\substack{\text{Matrix of elastic coeff.} \\ \text{with no Poisson effect}}} + \underbrace{\mathbf{D}^\nu(\nu)}_{\substack{\text{Matrix of elastic coeff.} \\ \text{with Poisson effect}}} \quad (15)$$

The implementation of this element accounts for distorted initial configuration and the possibility of defining orthotropic materials. More details on these ANCF element features are given in Section 4.

4 Bilinear ANCF Shell Element

Chrono's users may find detailed descriptions of the Chrono's laminated ANCF implementation in Refs. [9, 11].

The basic kinematics of the absolute nodal coordinate formulation (ANCF) shell finite element implemented in Chrono is depicted in Fig.3. The nodal position is defined as a function of the global position and the transverse gradient vector $\mathbf{r}_z^i = \frac{\partial \mathbf{r}^i}{\partial z^i}(\xi^i, \eta^i)$ which describes the orientation of the cross section. Element i 's positions and gradients on the mid-plane can be fully described as

$$\mathbf{r}_m^i(\xi^i, \eta^i) = \mathbf{S}_m^i(\xi^i, \eta^i) \mathbf{e}_p^i, \quad \frac{\partial \mathbf{r}^i}{\partial z^i}(\xi^i, \eta^i) = \mathbf{S}_m^i(\xi^i, \eta^i) \mathbf{e}_g^i, \quad (16)$$

where ξ^i and η^i refer to element i 's local, adimensional coordinates in the parametric space, $\mathbf{S}_m^i = [S_1^i \mathbf{I} \ S_2^i \mathbf{I} \ S_3^i \mathbf{I} \ S_4^i \mathbf{I}]$ is a bilinear shape function matrix, $\mathbf{e}_p^{ik} = \mathbf{r}^{ik}$ is the position vector of node k of element i , and $\mathbf{e}_g^{ik} = \partial \mathbf{r}^{ik} / \partial z^i$ is the position vector gradient of node k of element i (current and reference coordinates –taken from the initial configuration– are stored in the

ANCF shell element. The bilinear shape functions of the ANCF shell element are given by the following expressions

$$S_1^i = \frac{1}{4}(1 - \xi^i)(1 - \eta^i), S_2^i = \frac{1}{4}(1 + \xi^i)(1 - \eta^i),$$

$$S_3^i = \frac{1}{4}(1 + \xi^i)(1 + \eta^i), \text{ and } S_4^i = \frac{1}{4}(1 - \xi^i)(1 + \eta^i).$$

Note that shape functions, position vector gradients, angles, transformation matrices, intermediate operations between frames of reference, and strains are adimensional. The position of an arbitrary point in the shell may be described as

$$\mathbf{r}^i(x^i, y^i, z^i) = \mathbf{S}^i(x^i, y^i, z^i)\mathbf{e}^i, \quad (17)$$

where the combined shape function matrix is given by $\mathbf{S}^i = [\mathbf{S}_m^i \ z^i \mathbf{S}_m^i]$. Similarly, the coordinates of the element may be grouped as $\mathbf{e}^i = [(\mathbf{e}_p^i)^T \ (\mathbf{e}_g^i)^T]^T$. Note that Eq. (17) incorporates the element parametric coordinate along the element thickness z^i . Relying on

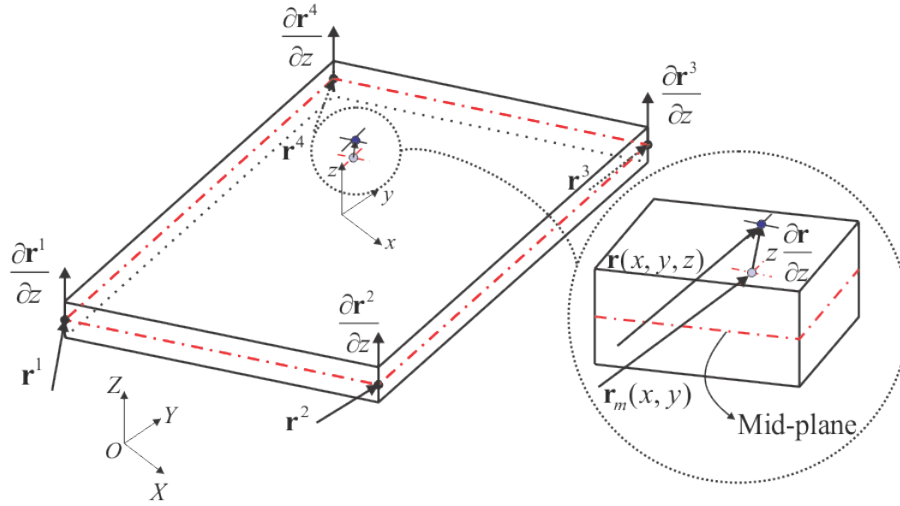


Figure 3: ANCF shell element's kinematic description

this kinematic description of the shell element, the Green-Lagrange strain tensor may be calculated as

$$\mathbf{E}^i = \frac{1}{2} \left((\mathbf{F}^i)^T \mathbf{F}^i - \mathbf{I} \right), \quad (18)$$

where \mathbf{F}^i is the deformation gradient matrix defined as the current configuration over the reference configuration. Using the current absolute nodal coordinates, this matrix may be defined as

$$\mathbf{F}^i = \frac{\partial \mathbf{r}^i}{\partial \mathbf{X}^i} = \frac{\partial \mathbf{r}^i}{\partial \mathbf{x}^i} \left(\frac{\partial \mathbf{X}^i}{\partial \mathbf{x}^i} \right)^{-1} \quad (19)$$

The strain tensor can then expressed in vector form in the following manner

$$\boldsymbol{\varepsilon}^i = [\varepsilon_{xx}^i \quad \varepsilon_{yy}^i \quad \gamma_{xy}^i \quad \varepsilon_{zz}^i \quad \gamma_{xz}^i \quad \gamma_{yz}^i]^T \quad (20)$$

where $\boldsymbol{\varepsilon}^i$ is the engineering strain vector in the deformed configuration, computed in Chrono. Strain derivatives are calculated in order to obtain generalized forces and an internal damping contribution. The elastic internal forces are spatially integrated over the element volume using Gaussian quadrature:

$$\mathbf{Q}_k^i = - \int_{V_0} \left(\frac{\partial \varepsilon^c}{\partial \mathbf{e}^i} \right) \frac{\partial W^i(\varepsilon^c + \varepsilon^{EAS})}{\partial \varepsilon^i} dV_0 \quad (21)$$

where ε^c is the compatible strain, obtained from the displacement field using ‘‘Assumed Natural Strain’’ interpolation to avoid transver/in-plane shear. Further, the term $W^i(\varepsilon^c + \varepsilon^{EAS})$ denotes the strain energy density function, which must be obtained by adding an enhanced strain contribution, ε^{EAS} . The second Piola–Kirchhoff stress tensor is obtained from the relation $\sigma^i = \frac{\partial W^i(\varepsilon^c + \varepsilon^{EAS})}{\partial \varepsilon^i}$. The addition of assumed natural strains and enhanced strains finds justifications of the mixed variational principle by Hu–Washizu [1].

4.1 Computation of Strains for Curved, Orthotropic Shells

Chrono allows the user to create initial geometries that will be automatically considered as ‘‘reference’’ by using covariant transformations. This is internally carried out in the implementation of the element. A frame of reference in the initial (reference) configuration is written as

$$(\mathbf{g}_0)_1 = (\mathbf{r}_0)_x = \frac{\partial \mathbf{r}_0}{\partial x}, \quad (\mathbf{g}_0)_2 = (\mathbf{r}_0)_y = \frac{\partial \mathbf{r}_0}{\partial y}, \quad (\mathbf{n}_0) = (\mathbf{r}_0)_z = \frac{\partial \mathbf{r}_0}{\partial z}. \quad (22)$$

where subscript 0 denotes initial. The unit base vectors of the local Cartesian frame may be obtained as

$$(\mathbf{e}_0)_1 = \frac{(\mathbf{g}_0)_1}{|(\mathbf{g}_0)_1|}, \quad (\mathbf{e}_0)_3 = \mathbf{n}_0, \quad (\mathbf{e}_0)_2 = (\mathbf{e}_0)_3 \times (\mathbf{e}_0)_1. \quad (23)$$

For orthotropic materials, the mechanical behavior depends on fiber orientations. For this reason, it is necessary to include fiber angle in the definition of the local Cartesian frame. Assuming that θ represents the fiber angle with respect to the X axis of the previously calculated local Cartesian frame, the new basis takes the following form:

$$\begin{aligned} (\mathbf{e}_0)_1^{Or} &= (\mathbf{e}_0)_1 \cos \theta + (\mathbf{e}_0)_2 \sin \theta, \\ (\mathbf{e}_0)_2^{Or} &= -(\mathbf{e}_0)_1 \sin \theta + (\mathbf{e}_0)_2 \cos \theta, \quad (\mathbf{e}_0)_3^{Or} = (\mathbf{e}_0)_3. \end{aligned} \quad (24)$$

The relation between the two covariant base vectors may be expressed as

$$(\mathbf{g}_0)_{i'} = \beta_{i'}^j (\mathbf{e}_0)_{1,j}^{Or}, \quad (25)$$

where scalars β_{ij}^j are obtained via a dot product between two dimensional vectors. In matrix form, the coefficients of contravariance transformation may be obtained from the Jacobian of the position vectors at the reference configuration and the local Cartesian frame including anisotropy in the following form

$$\boldsymbol{\beta} = \begin{bmatrix} \mathbf{Y}^{-1}|_{C1}^T \\ \mathbf{Y}^{-1}|_{C2}^T \\ \mathbf{Y}^{-1}|_{C3}^T \end{bmatrix} [(\mathbf{e}_0)_1 \quad (\mathbf{e}_0)_2 \quad (\mathbf{e}_0)_3] \quad (26)$$

where $\mathbf{Y}^{-1}|_{C_i}$ is the i column of the inverse of $\mathbf{Y} = \frac{\partial \mathbf{r}}{\partial \mathbf{x}} = [(\mathbf{g}_0)_1 \quad (\mathbf{g}_0)_2 \quad \mathbf{n}_0]$. The components of the 3-by-3 matrix $\boldsymbol{\beta}$ are used to set up a transformation matrix necessary for the calculation of strains:

$$\boldsymbol{\beta} = \begin{bmatrix} \beta_{11} & \beta_{12} & \beta_{13} \\ \beta_{21} & \beta_{22} & \beta_{23} \\ \beta_{31} & \beta_{32} & \beta_{33} \end{bmatrix} \quad (27)$$

where $\beta_{ij} = \beta(i, j)$. Finally the compatible strains are calculated as:

$$\boldsymbol{\varepsilon} = \frac{1}{2} \boldsymbol{\beta}^T \left(\begin{bmatrix} g_{11} & g_{12} & g_{13} \\ g_{21} & g_{22} & g_{23} \\ g_{31} & g_{32} & g_{33} \end{bmatrix} - \begin{bmatrix} (g_0)_{11} & (g_0)_{12} & (g_0)_{13} \\ (g_0)_{21} & (g_0)_{22} & (g_0)_{23} \\ (g_0)_{31} & (g_0)_{32} & (g_0)_{33} \end{bmatrix} \right) \boldsymbol{\beta} = \begin{bmatrix} \varepsilon_{11} & \varepsilon_{12} & \varepsilon_{13} \\ \varepsilon_{21} & \varepsilon_{22} & \varepsilon_{23} \\ \varepsilon_{31} & \varepsilon_{32} & \varepsilon_{33} \end{bmatrix}, \quad (28)$$

where $g_{ij} = \mathbf{g}_i \cdot \mathbf{g}_j$ and $(g_0)_{ij} = (\mathbf{g}_0)_i \cdot (\mathbf{g}_0)_j$.

4.2 ANCF Shell Element Implementation

4.2.1 Initial Steps

Chrono calls the method `MyForce::Evaluate` to evaluate the internal forces of the shell element at one Gauss point. The orientations and contravariant vectors are computed in order to perform calculation of strains as orthotropic material which may an initially curved configuration.

4.2.2 Locking Remedies - Enhanced Assumed Strain

The Enhanced Assumed Strain (EAS) is added to the compatible strain in order to alleviate transverse shear locking. From Eq. (19), we can define the following matrix \mathbf{J}^i , which relates the initial and reference configuration:

$$\mathbf{J}^i = \frac{\partial \mathbf{X}^i}{\partial \mathbf{x}^i}, \quad (29)$$

where \mathbf{J}^i is the inverse of the deformation gradient and is used to construct a constant transformation matrix (note that \mathbf{J}^i only depends on the initial and reference configuration).

$$\mathbf{T}^i = \begin{bmatrix} (J_{11}^i)^2 & (J_{12}^i)^2 & 2J_{11}^i J_{12}^i & (J_{13}^i)^2 & 2J_{11}^i J_{13}^i & 2J_{12}^i J_{13}^i \\ (J_{21}^i)^2 & (J_{22}^i)^2 & 2J_{21}^i J_{22}^i & (J_{23}^i)^2 & 2J_{21}^i J_{23}^i & 2J_{22}^i J_{23}^i \\ J_{11}^i J_{21}^i & J_{12}^i J_{22}^i & J_{11}^i J_{22}^i + J_{12}^i J_{21}^i & J_{13}^i J_{23}^i & J_{11}^i J_{23}^i + J_{13}^i J_{21}^i & J_{12}^i J_{23}^i + J_{13}^i J_{22}^i \\ (J_{31}^i)^2 & (J_{32}^i)^2 & 2J_{31}^i J_{32}^i & (J_{33}^i)^2 & 2J_{31}^i J_{33}^i & 2J_{32}^i J_{33}^i \\ J_{11}^i J_{31}^i & J_{12}^i J_{32}^i & J_{11}^i J_{32}^i + J_{12}^i J_{31}^i & J_{13}^i J_{33}^i & J_{11}^i J_{33}^i + J_{13}^i J_{31}^i & J_{12}^i J_{33}^i + J_{13}^i J_{32}^i \\ J_{21}^i J_{31}^i & J_{22}^i J_{32}^i & J_{21}^i J_{32}^i + J_{22}^i J_{31}^i & J_{23}^i J_{33}^i & J_{21}^i J_{33}^i + J_{23}^i J_{31}^i & J_{22}^i J_{33}^i + J_{23}^i J_{32}^i \end{bmatrix} \quad (30)$$

The interpolation matrix for the distribution of the in-plane strains is defined as

$$\mathbf{N}(\xi) = \begin{bmatrix} \xi & 0 & 0 & 0 & 0 \\ 0 & \eta & 0 & 0 & 0 \\ 0 & 0 & \xi & \eta & 0 \\ 0 & 0 & 0 & 0 & \zeta \\ 0 & 0 & 0 & 0 & 0 \\ 0 & 0 & 0 & 0 & 0 \end{bmatrix} \quad (31)$$

This matrix guarantees that $\int \mathbf{N}(\xi) d\xi = \mathbf{0}$. The following 6-by-5 matrix is defined to include the enhanced assumed strain in the internal forces:

$$\mathbf{G}(\xi) = \frac{|\mathbf{J}_0|}{|\mathbf{J}(\xi)|} \mathbf{T}_0^{-T} \mathbf{N}(\xi), \quad (32)$$

where \mathbf{T}_0 is a constant transformation matrix obtained by evaluating \mathbf{T} at the center of the element in the reference configuration. With the aid of a vector of internal parameters α , the EAS may be calculated as

$$\boldsymbol{\varepsilon}^{EAS}(\xi) = \mathbf{G}(\xi) \boldsymbol{\alpha}. \quad (33)$$

The total strain will be the addition of the compatible strain and the EAS, as follows

$$\boldsymbol{\varepsilon} = \boldsymbol{\varepsilon}^c + \boldsymbol{\varepsilon}^{EAS} \quad (34)$$

The EAS strain is a function of the \mathbf{G} matrix at each Gaussian integration point and the vector of internal parameters $\boldsymbol{\alpha}$, which is calculated by solving iteratively the equation $\mathbf{h}^i(\mathbf{e}^i, \alpha^i) = \int_{V_0^i} \left(\frac{\partial \boldsymbol{\varepsilon}^{EAS}}{\partial \alpha^i} \right)^T \frac{\partial \mathbf{W}^i(\boldsymbol{\varepsilon}^c + \boldsymbol{\varepsilon}^{EAS})}{\partial \boldsymbol{\varepsilon}^i} dV_0^i = \mathbf{0}$. The values of \mathbf{h}^i , $\frac{\partial \mathbf{h}_n}{\partial \alpha_n}$, and $\frac{\partial \mathbf{h}_n}{\partial \mathbf{e}_n}$ are computed within the Gaussian integration loop. The updated value of $\boldsymbol{\alpha}$ in the current iteration is defined by $\boldsymbol{\alpha}_{n+1} = \boldsymbol{\alpha}_n - \left(\frac{\partial \mathbf{h}_n}{\partial \boldsymbol{\alpha}_n} \right)^{-1} \left(\mathbf{h}_n + \frac{\partial \mathbf{h}_n}{\partial \mathbf{e}_n} \Delta \mathbf{e}_{n+1} \right)$.

4.2.3 Locking Remedies - Assumed Natural Strain

Assumed natural strains (ANS) are introduced in Chrono's implementation to avoid shear and thickness locking in the shell finite element. Compatible thickness and shear strains, which are interpolated in the computation of internal forces. Additional sampling points A, B, C, and D, located at the middle of the element edges, are used to calculate the ANS strain as follows

$$\boldsymbol{\varepsilon}_{zz}^{ANS} = S_1^{ANS} \boldsymbol{\varepsilon}_{zz}^1 + S_2^{ANS} \boldsymbol{\varepsilon}_{zz}^2 + S_3^{ANS} \boldsymbol{\varepsilon}_{zz}^3 + S_4^{ANS} \boldsymbol{\varepsilon}_{zz}^4 \quad (35)$$

$$\tilde{\gamma}_{xz}^{ANS} = \frac{1}{2} (1 - \eta) \tilde{\gamma}_{xz}^C + \frac{1}{2} (1 + \eta) \tilde{\gamma}_{xz}^D \quad (36)$$

$$\tilde{\gamma}_{yz}^{ANS} = \frac{1}{2} (1 - \xi) \tilde{\gamma}_{yz}^A + \frac{1}{2} (1 + \xi) \tilde{\gamma}_{yz}^B, \quad (37)$$

where tildes denote covariant quantities.

4.2.4 Equations of Motion

The mass matrix of the element is given by

$$\mathbf{M}^i = \int_{V_o^i} \rho_0^i (\mathbf{S}^i)^T \mathbf{S}^i dV_o^i, \quad (38)$$

which remains constant throughout the simulation. The equations of motion may be written as

$$\mathbf{M}^i \ddot{\mathbf{e}}^i = \mathbf{Q}_k^i(\mathbf{e}^i, \dot{\mathbf{e}}^i, \alpha^i) + \mathbf{Q}_e^i(\mathbf{e}^i, \dot{\mathbf{e}}^i, t), \quad (39)$$

where \mathbf{Q}_k is the element elastic force vector and \mathbf{Q}_e is the external force vector. The Newton differences for \mathbf{e}_{n+1} and α_{n+1} are calculated by solving the following system of equations

$$\begin{bmatrix} \partial \mathbf{f} / \partial \mathbf{e}_n & \partial \mathbf{f} / \partial \alpha_n \\ \partial \mathbf{h} / \partial \mathbf{e}_n & \partial \mathbf{h} / \partial \alpha_n \end{bmatrix} \begin{bmatrix} \Delta \mathbf{e}_{n+1} \\ \Delta \alpha_{n+1} \end{bmatrix} = - \begin{bmatrix} \mathbf{f}_n \\ \mathbf{h}_n \end{bmatrix}. \quad (40)$$

After eliminating $\Delta \alpha_{n+1}$ the following equation can solve for $\Delta \mathbf{e}_{n+1}$ using the following equation:

$$\left(\frac{\partial \mathbf{f}_n}{\partial \mathbf{e}_n} - \frac{\partial \mathbf{f}_n}{\partial \alpha_n} \left(\frac{\partial \mathbf{h}_n}{\partial \alpha_n} \right)^{-1} \frac{\partial \mathbf{h}_n}{\partial \mathbf{e}_n} \right) \Delta \mathbf{e}_{n+1} = -\mathbf{f}_n + \frac{\partial \mathbf{f}_n}{\partial \alpha_n} \left(\frac{\partial \mathbf{h}_n}{\partial \alpha_n} \right)^{-1} \mathbf{h}_n. \quad (41)$$

4.3 Computation of the Jacobian of the Elastic Forces

The Jacobian of the elastic forces are calculated in `MyJacobian::Evaluate`. The method for Jacobian of elastic forces recalculates many of the quantities involved in the computation of internal forces. This is done this way in order to effectively separate the both calculations and allow for single computation of the Jacobian in each time step (in the future). Basic quantities related to the ANCF shell element internal forces are recalculated for the calculation of the Jacobian.

The Jacobian of the elastic forces is split into different parts:

Jacobian of elastic forces Direct derivation of generalized elastic forces w.r.t. coordinates (Eq. (21)).

Jacobian of EAS forces The Jacobian of the generalized forces coming from the EAS formulation.

The computation of the Jacobian of the elastic forces is called for each layer of material. The total Jacobian, for all the layers of the element, is accumulated if the element features more than one layer.

5 Validation of Cable Element

This section shows the results of a validation effort for Chrono’s ANCF beam element. The example tested has been extracted from [4] and validates this finite element’s elastic force formulation. Additionally, it checks the application of distributed gravity and initial conditions. This validation is performed in Chrono’s unit test: [test_ANCFBeam.cpp](#).

5.1 Model’s Definition

The model used for validating Chrono’s implementation is taken from subsection 7.2 of the manuscript [4]. It consists of a beam composed of four finite elements which has one end constrained to the ground through a spherical joint. An initial angular velocity of 4 rad/s about the vertical Y axis is applied by imposing the corresponding initial linear velocity along the X axis. A sketch of the model is shown in Fig.4. The parameters of this model are implemented as in [4], i.e., dependent on a parameter f . Thus, the pendulum length is length 1 m, cross-section area $10^{-6}f^2$ m², density $8000/f^2$ kg/m³, and Young’s modulus $10^9/f^4$ N/m². Poisson’s ratio is assumed to be zero and the effect of gravity (z-direction) is considered. The study shown in this report is performed with $f = 5$.

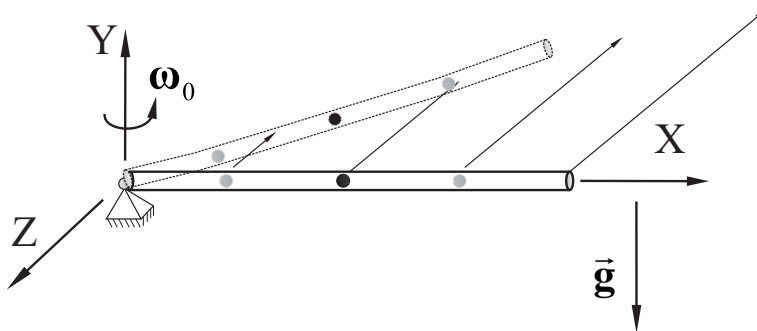


Figure 4: ANCF beam element validation model

5.2 Numerical Validation

The three-dimensional pendulum example’s results from subsection 7.2 of Ref. [4] were digitized and compare with the results of Chrono’s test [test_ANCFBeam.cpp](#), in the Chrono::FEA module. The results may be observed in Figs. 5 and 6. The results show good agreement between published results and Chrono’s output. It must be noted that the bending strain formula used in Chrono is that presented in [4] since others have been proposed [3].

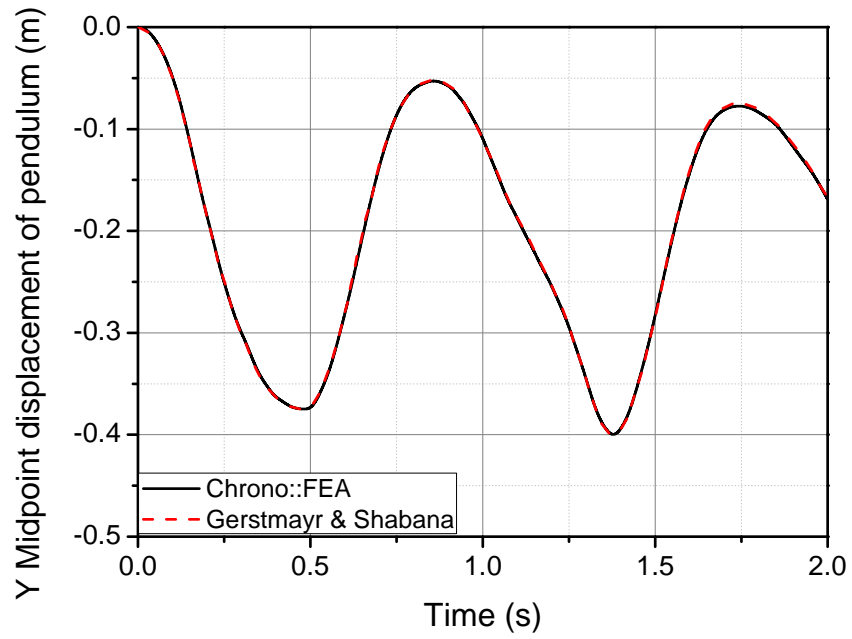


Figure 5: ANCF beam element verification on the vertical displacement

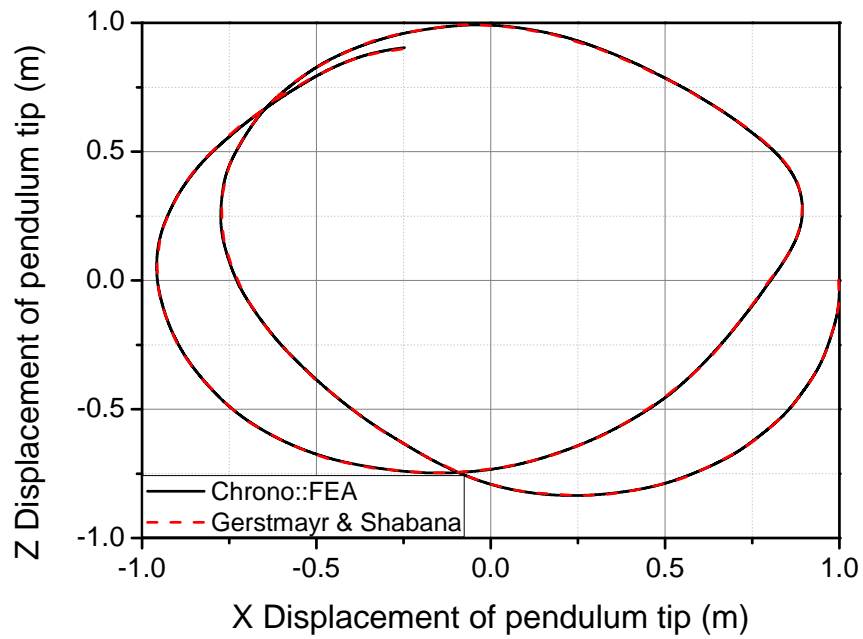


Figure 6: ANCF beam element verification on the horizontal plane

6 Validation of Beam Element

The shear deformable beam element in **Chrono** has been verified against the results of [6]. Specifically, the example 4.1 for both small and large deformation was used. The setup for this comparison may be found in the unit test [utest_ANCFBeam.cpp](#). Note that the internal force formulation tested is the one based on a fully three-dimensional continuum mechanics approach, where reduced integration of Poisson ratio terms is used to avoid volumetric locking.

7 Validation of the ANCF Shell Element

In this section we validate the implementation of **Chrono** 's absolute nodal coordinate shell element using commercial software.

7.1 Validation of the Isotropic Implementation

This subsection shows some results of the validation of the elastic, isotropic implementation of a four-node shell element implemented in **Chrono** . This nonlinear finite element uses absolute nodal coordinates to describe the position of the nodes and a vector normal to the shell surface.

7.1.1 Model's Definition

The first model chosen to verify **Chrono** 's implementation is a cantilever flat shell subjected to a sudden, constant load at a corner. Due to the application of a sudden load, the shell undergoes vibrations that are damped out by adding structural damping. The length, width, and thickness of the flat shell (plate) are assumed to be 1.0 m, 1.0 m, and 0.01 m, respectively. The Young modulus and Poisson ratio are 2.1×10^8 Pa and 0.3, respectively. A vertical force of 50N is applied downwards in the absence of a gravity field. Structural damping is purposely employed to bring the system to static equilibrium. More details on this example may be found in Ref. [11].

The details of this model and its corresponding results may be consulted and obtained running the unit test [test_ANCFShellIso.cpp](#), which is available in **Chrono** 's repository.

7.1.2 Numerical Validation

The time evolution for the system and loads defined in the previous subsection results in underdamped oscillations of the shell. Figure 7 displays the oscillations of the shell's loaded tip for two different mesh sizes.

Comparison is performed with the commercial software **ANSYS** to ensure that **Chrono** 's implementation converges to the correct displacement and at a good rate. Reference results are obtained from a 64x64 mesh in **ANSYS**. It must be emphasized that, while **ANSYS**'s results are obtained from static, finite strain results, **Chrono** performs dynamic simulations to find the static equilibrium position. Convergence results are plotted in Fig. 8.

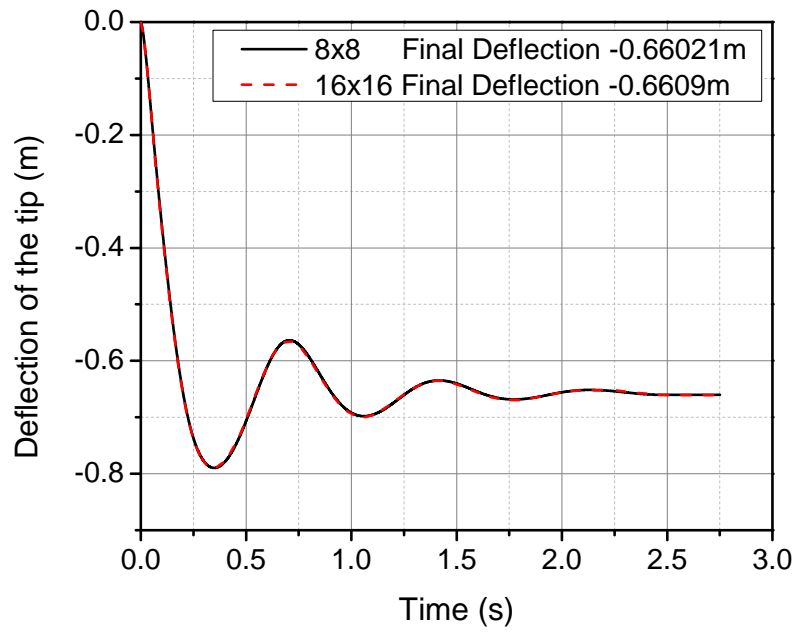


Figure 7: Tip vertical coordinate time evolution

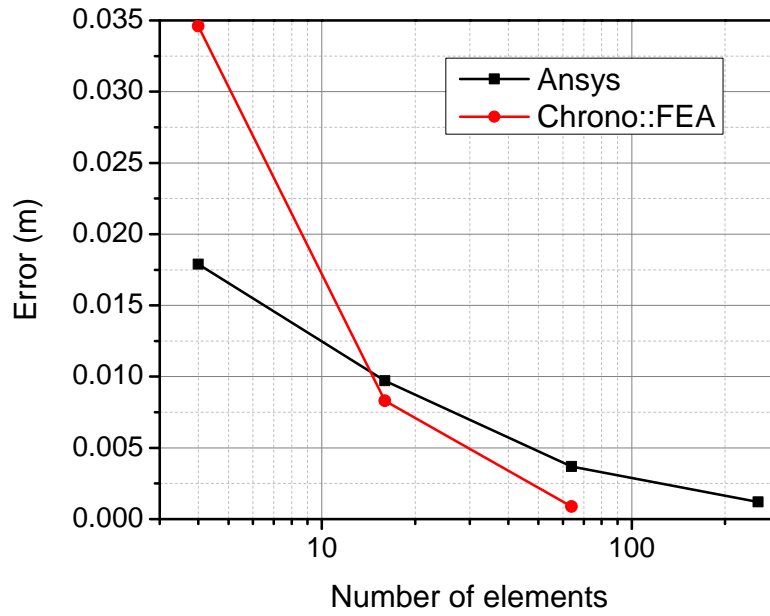


Figure 8: Convergence rate comparison

7.2 Validation of the Orthotropic Implementation

Chrono allows the user to create laminated shell models using the absolute nodal coordinate formulation. A number of layers with different ply angles and orthotropic elastic constants may be selected. Laminated shell elements have many applications in mechanical engineering problems and, for example, may be used in **Chrono** to model fully dynamic models of tires.

7.2.1 Model's Definition

To validate the laminated shell implementation in **Chrono**, we have chosen to monitor the response of a quarter of a cylindrical shell. This cylindrical shell is laying in horizontal position with its longitudinal Y axis constrained to the ground at $X = 0$. A load of -10 N is applied at a corner of the free end. Some parameters of the shell geometry are taken as follows: Y length, 1.0 m, single layer thickness, 0.005 m, and cylinder radius, 1.0 m. Elastic constants are chosen in the following way: $E_x = 2.0 \times 10^8$ Pa, $E_y = E_z = 1.0 \times 10^8$ Pa, $\nu = 0.3$, and $G_{xy} = G_{yz} = G_{xz} = 3.84615 \times 10^7$ Pa. The ANCF shell element is chosen to have two stacked layers with ply angles $+20^\circ$ and -20° [10].

This model is defined in **Chrono**'s [test_ANCFShellOrt.cpp](#).

7.2.2 Numerical Validation

A sudden force is applied at a free corner of the shell and underdamped motion follows. A reference solution for this problem is obtained in **ANSYS** using a 64×64 mesh of **Shell181** elements (with incompatible modes) and solving a large deformation static analysis: The vertical displacement (not position) for the loaded node is -0.80207 m. The steady state value for that node's displacement is obtained in **Chrono** by using structural damping to bring the system to equilibrium ($\alpha = 0.25$). When small oscillations are present in **Chrono**'s solution, the mean value of such an oscillation is taken as steady-state response. The time evolution of the loaded tip position for a 6×6 shell is plotted in Fig. 9 (a displacement of approximately -0.8 m may be observed). A convergence study is performed by comparing the steady state of **Chrono**'s simulation results and static solution. The results are shown in Fig. 10, where a displacement of -0.80207 m was taken as a reference.

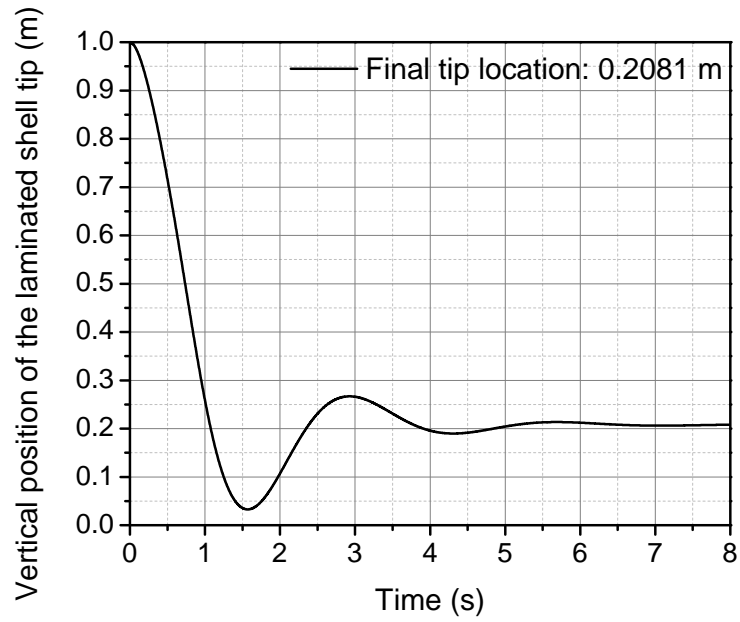


Figure 9: Loaded tip position under the application of sudden load of 10N

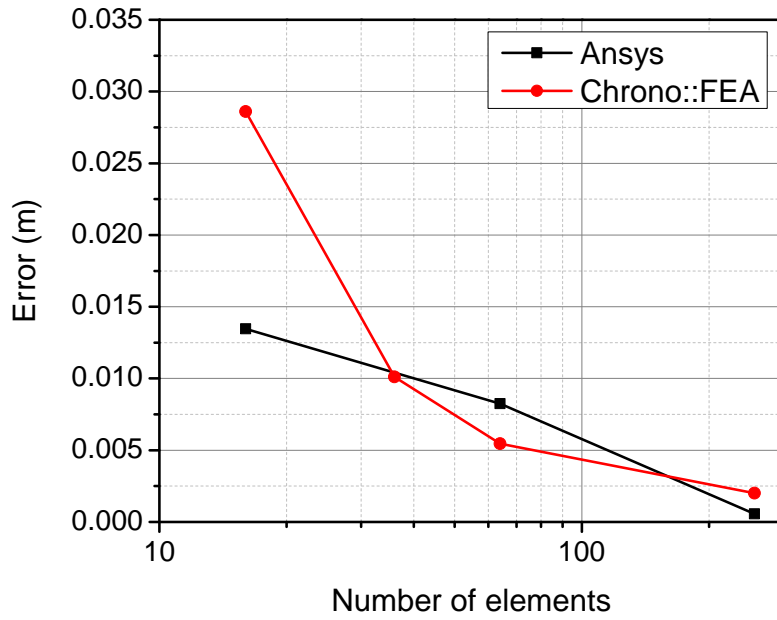


Figure 10: Convergence comparison: ANSYS and Chrono

References

- [1] U Andelfinger and E Ramm. Eas-elements for two-dimensional, three-dimensional, plate and shell structures and their equivalence to hr-elements. *International Journal for Numerical Methods in Engineering*, 36(8):1311–1337, 1993.
- [2] M Berzeri and AA Shabana. Development of simple models for the elastic forces in the absolute nodal co-ordinate formulation. *Journal of Sound and Vibration*, 235(4):539–565, 2000.
- [3] J. Gerstmayr and H. Irschik. On the correct representation of bending and axial deformation in the absolute nodal coordinate formulation with an elastic line approach. *Journal of Sound and Vibration*, 318 (3):461–487, 2008.
- [4] J. Gerstmayr and A.A. Shabana. Analysis of thin beams and cables using the absolute nodal co-ordinate formulation. *Nonlinear Dynamics*, 45(1):109–130, 2006.
- [5] Johannes Gerstmayr, Hiroyuki Sugiyama, and Aki Mikkola. Review on the absolute nodal coordinate formulation for large deformation analysis of multibody systems. *Journal of Computational and Nonlinear Dynamics*, 8(3):031016, 2013.
- [6] K. Nachbagauer, P. Gruber, and J. Gerstmayr. Structural and Continuum Mechanics Approaches for a 3D Shear Deformable ANCF Beam Finite Element: Application to Static and Linearized Dynamic Examples. *J. Comput. Nonlinear Dynam*, 8 (2):021004, 2012.
- [7] Ahmed A Shabana. Definition of the slopes and the finite element absolute nodal coordinate formulation. *Multibody System Dynamics*, 1(3):339–348, 1997.
- [8] Zhenxing Shen, Pei Li, Cheng Liu, and Gengkai Hu. A finite element beam model including cross-section distortion in the absolute nodal coordinate formulation. *Nonlinear Dynamics*, 77(3):1019–1033, 2014.
- [9] H. Yamashita, A. Valkeapaa, P. Jayakumar, and H. Sugiyama. Bi-linear shear deformable ANCF shell element using continuum mechanics approach. In *Proceedings of ASME International Conference on Multibody Systems, Nonlinear Dynamics, and Control, Buffalo, NY*. ASME, 2014.
- [10] Hiroki Yamashita, Yusuke Matsutani, and Hiroyuki Sugiyama. Longitudinal tire dynamics model for transient braking analysis: Ancf-lugre tire model. *Journal of Computational and Nonlinear Dynamics*, 10(3):031003, 2015.
- [11] Hiroki Yamashita, Antti I Valkeapää, Paramsothy Jayakumar, and Hiroyuki Sugiyama. Continuum mechanics based bilinear shear deformable shell element using absolute nodal coordinate formulation. *Journal of Computational and Nonlinear Dynamics*, 10(5):051012, 2015.